Class. Quantum Grav. **29** (2012) 025005 (10pp) doi:10.1088/0264-9381/29/2/025005

Characterization of the Virgo seismic environment

T Accadia[1], F Acernese[2ac], P Astone[3a], G Ballardin[4], F Barone[2ac], M Barsuglia[5], A Basti[6ab], Th S Bauer[7a], M Bebronne[1], M G Beker[7a], A Belletoile[1], M Bitossi[6a], M A Bizouard[8a], M Blom[7a], F Bondu[9b], L Bonelli[6ab], R Bonnand[10], V Boschi[6a], L Bosi[11a], B Bouhou[5], S Braccini[6a], C Bradaschia[6a], M Branchesi[12ab], T Briant[13], A Brillet[9a], V Brisson[8a], T Bulik[14bc], H J Bulten[7ab], D Buskulic[1], C Buy[5], G Cagnoli[12a], E Calloni[2ab], B Canuel[4], F Carbognani[4], F Cavalier[8a], R Cavalieri[4], G Cella[6a], E Cesarini[12b], O Chaibi[9a], E Chassande-Mottin[5], A Chincarini[15], A Chiummo[4], F Cleva[9a], E Coccia[16ab], P-F Cohadon[13], C N Colacino[6ab], J Colas[4], A Colla[3ab], M Colombini[3b], A Conte[3ab], M Coughlin[17], J-P Coulon[9a], E Cuoco[4], S D'Antonio[16a], V Dattilo[4], M Davier[8a], R Day[4], R De Rosa[2ab], G Debreczeni[18], W Del Pozzo[7a], M del Prete[19b], L Di Fiore[2a], A Di Lieto[6ab], M Di Paolo Emilio[16ac], A Di Virgilio[6a], A Dietz[1], M Drago[19ab], G Endrőczi[18], V Fafone[16ab], I Ferrante[6ab], F Fidecaro[6ab], I Fiori[4], R Flaminio[10], L A Forte[2a], J-D Fournier[9a], J Franc[10], S Frasca[3ab], F Frasconi[6a], M Galimberti[10], L Gammaitoni[11ab], F Garufi[2ab], M E Gáspár[18], G Gemme[15], E Genin[4], A Gennai[6a], A Giazotto[6a], R Gouaty[1], M Granata[5], C Greverie[9a], G M Guidi[12ab], J-F Hayau[9b], A Heidmann[13], H Heitmann[9], P Hello[8a], P Jaranowski[14d], I Kowalska[14b], A Królak[14ae], N Leroy[8a], N Letendre[1], T G F Li[7a], N Liguori[19ab], M Lorenzini[12a], V Loriette[8b], G Losurdo[12a], E Majorana[3a], I Maksimovic[8b], N Man[9a], M Mantovani[6ac], F Marchesoni[11a], F Marion[1], J Marque[4], F Martelli[12ab], A Masserot[1], C Michel[10], L Milano[2ab], Y Minenkov[16a], M Mohan[4], N Morgado[10], A Morgia[16ab], S Mosca[2ab], B Mours[1], L Naticchioni[3ab], F Nocera[4], G Pagliaroli[16ac], L Palladino[16ac], C Palomba[3a], F Paoletti[4,6a], M Parisi[2ab], A Pasqualetti[4], R Passaquieti[6ab], D Passuello[6a], G Persichetti[2ab], F Piergiovanni[12ab], M Pietka[14d], L Pinard[10], R Poggiani[6ab], M Prato[15], G A Prodi[19ab], M Punturo[11a], P Puppo[3a], D S Rabeling[7ab], I Rácz[18], P Rapagnani[3ab], V Re[16ab], T Regimbau[9a], F Ricci[3ab], F Robinet[8a], A Rocchi[16a], L Rolland[1], R Romano[2ac], D Rosińska[14cf], P Ruggi[4], B Sassolas[10], D Sentenac[4], L Sperandio[16ab], R Sturani[12ab], B Swinkels[4], M Tacca[4], L Taffarello[19c], A Toncelli[6ab], M Tonelli[6ab], O Torre[6ac], E Tournefier[1], F Travasso[11ab], G Vajente[6ab], J F J van den Brand[7ab], C Van Den Broeck[7a], S van der Putten[7a], M Vasuth[18], M Vavoulidis[8a], G Vedovato[19c], D Verkindt[1], F Vetrano[12ab], A Viceré[12ab], J-Y Vinet[9a], S Vitale[7a], H Vocca[11a], R L Ward[5], M Was[8a], M Yvert[1], A Zadrożny[14e] and J-P Zendri[19c]

[1] Laboratoire d'Annecy-le-Vieux de Physique des Particules (LAPP), Université de Savoie, CNRS/IN2P3, F-74941 Annecy-Le-Vieux, France

[2] INFN, Sezione di Napoli[a]; Università di Napoli 'Federico II'[b] Complesso Universitario di Monte S. Angelo, I-80126 Napoli; Università di Salerno, Fisciano, I-84084 Salerno[c], Italy

[3] INFN, Sezione di Roma[a]; Università 'La Sapienza'[b], I-00185 Roma, Italy
[4] European Gravitational Observatory (EGO), I-56021 Cascina (PI), Italy
[5] Laboratoire AstroParticule et Cosmologie (APC) Université Paris Diderot, CNRS: IN2P3, CEA: DSM/IRFU, Observatoire de Paris, 10 rue A. Domon et L. Duquet, 75013 Paris - France
[6] INFN, Sezione di Pisa[a]; Università di Pisa[b]; I-56127 Pisa; Università di Siena, I-53100 Siena[c], Italy
[7] Nikhef, Science Park, Amsterdam, the Netherlands[a]; VU University Amsterdam, De Boelelaan 1081, 1081 HV Amsterdam, the Netherlands[b]
[8] LAL, Université Paris-Sud, IN2P3/CNRS, F-91898 Orsay[a]; ESPCI, CNRS, F-75005 Paris[b], France
[9] Université Nice-Sophia-Antipolis, CNRS, Observatoire de la Côte d'Azur, F-06304 Nice[a]; Institut de Physique de Rennes, CNRS, Université de Rennes 1, 35042 Rennes[b], France
[10] Laboratoire des Matériaux Avancés (LMA), IN2P3/CNRS, F-69622 Villeurbanne, Lyon, France
[11] INFN, Sezione di Perugia[a]; Università di Perugia[b], I-06123 Perugia, Italy
[12] INFN, Sezione di Firenze, I-50019 Sesto Fiorentino[a]; Università degli Studi di Urbino 'Carlo Bo', I-61029 Urbino[b], Italy
[13] Laboratoire Kastler Brossel, ENS, CNRS, UPMC, Université Pierre et Marie Curie, 4 Place Jussieu, F-75005 Paris, France
[14] IM-PAN 00-956 Warsaw[a]; Astronomical Observatory Warsaw University 00-478 Warsaw[b]; CAMK-PAN 00-716 Warsaw[c]; Białystok University 15-424 Białystok[d]; IPJ 05-400 Świerk-Otwock[e]; Institute of Astronomy 65-265 Zielona Góra[f], Poland
[15] INFN, Sezione di Genova; I-16146 Genova, Italy
[16] INFN, Sezione di Roma Tor Vergata[a]; Università di Roma Tor Vergata, I-00133 Roma[b]; Università dell'Aquila, I-67100 L'Aquila[c], Italy
[17] Physics and Astronomy, Carleton College, Northfield, MN, 55057, USA
[18] RMKI, H-1121 Budapest, Konkoly Thege Miklós út 29-33, Hungary
[19] INFN, Gruppo Collegato di Trento[a] and Università di Trento[b], I-38050 Povo, Trento, Italy; INFN, Sezione di Padova[c] and Università di Padova[d], I-35131 Padova, Italy

E-mail: coughlim@carleton.edu

Received 9 August 2011, in final form 25 November 2011
Published 21 December 2011
Online at stacks.iop.org/CQG/29/025005

Abstract

The Virgo gravitational wave detector is an interferometer (ITF) with 3 km arms located in Pisa, Italy. From July to October 2010, Virgo performed its third science run (VSR3) in coincidence with the LIGO detectors. Despite several techniques adopted to isolate the ITF from the environment, seismic noise remains an important issue for Virgo. Vibrations produced by the detector infrastructure (such as air conditioning units, water chillers/heaters, pumps) are found to affect Virgo's sensitivity, with the main coupling mechanisms being through beam jitter and scattered light processes. The Advanced Virgo design seeks to reduce ITF couplings to environmental noise by having most vibration-sensitive components suspended and in vacuum, as well as muffle and relocate loud machines. During the months of June and July in 2010, a Güralp-3TD seismometer was stationed at various locations around the Virgo site hosting major infrastructure machines. Seismic data were examined using spectral and coherence analysis with seismic probes close to the detector. The primary aim of this study was to identify noisy machines which seismically affect the ITF environment and thus require mitigation attention. Analyzed machines are located at various distances from the experimental halls, ranging from 10 to 100 m. An attempt is made to measure the attenuation of emitted noise at

the ITF and correlate it with the distance from the source and with seismic attenuation models in soil.

PACS numbers: 04.80.Nn, 07.05.Kf, 95.55.Ym

(Some figures may appear in colour only in the online journal)

1. Introduction

The general theory of relativity predicts that all accelerating objects with non-symmetric mass distributions produce gravitational waves (GW)[20]. LIGO (the Laser Interferometer Gravitational-Wave Observatory) [1] and Virgo [2] experiments seek to directly detect GWs and use them to study astrophysical sources.

Virgo, located in Cascina, Italy, consists of a laser Michelson interferometer with 3 km long, Fabry–Perot resonant optical cavities in its arms. With respect to other similar detectors, Virgo has enhanced sensitivity between 10 and 100 Hz due to the seismic isolation performance of the 'super-attenuators' to which the test masses are suspended [3]. Beginning in 2011, the detector expects to undergo upgrades, known as Advanced Virgo (AdV), to improve its sensitivity by one order of magnitude [4].

Seismic noise places a limit on Virgo's detection sensitivity. In particular, the main source of seismic noise in the 10–100 Hz band at the Virgo site is the detector's infrastructure machines (see figure 1 (left) for a comparison with a low-noise model). Although Virgo's mirrors are well isolated from a local seismic activity by suspension systems made up of multi-stage pendulums, seismic noise remains a concern. The residual ground motion causes 'diffused light' [5]. Because of unavoidable imperfections in the detector's optical components, some tiny fraction of light can exit the main optical path and strike a surface that is connected to the ground, and thus be subject to the local seismic field. When this light scatters off objects connected to the ground (such as optical components on external tables used for detector controls), it is often diffused over a wide solid angle. A fraction of the light can re-enter the main beam path, but with a noisy phase modulated by the seismically excited scattering object. This phenomenon functions as additional noise in the GW channel and limits its sensitivity.

Because seismic events couple in this way into the GW channel, it is necessary to understand and attenuate the noise from the local seismic environment. Many of the strong lines seen during VSR2 can be attributed to seismic sources (see figure 1 (right)). To assist in the identification effort, the Virgo detector is supplemented with several types of environmental sensors, including seismometers and accelerometers, that monitor the local environment [6]. These channels are used to detect environmental disturbances that can couple to the GW channel and are placed in sensitive areas of the interferometer. To reduce the influence of anthropogenic noise, during the AdV upgrade, machines that are identified as seismically and acoustically affecting the interferometer will be replaced, moved, or isolated [4]. The current proposal is to move all chillers, water pumps, air compressors, and air conditioners from their current locations to other areas farther from the interferometer. By placing these machines on their own isolated platforms and by adopting techniques to reduce noise emission and propagation, Virgo hopes to significantly reduce their effects on the detector. To prioritize the actions required to reduce noise at Virgo, a careful documentation of the present local

[20] As presented at the Gravitational-Wave Physics and Astronomy Workshop in Milwaukee, Wisconsin, 26–29 January, 2011.

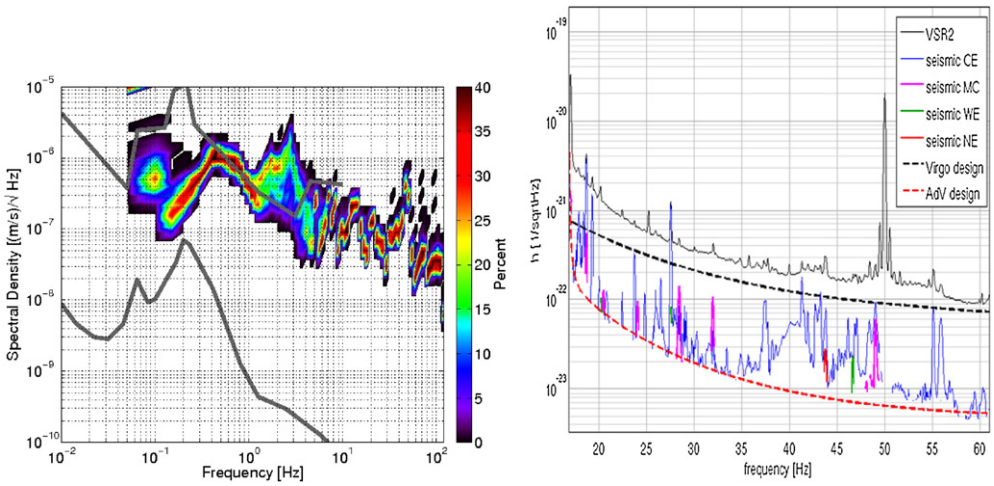

Figure 1. Left: variation in the root spectral density of the Güralp seismometer at the Virgo site during a day in June 2010. The two solid curves correspond to the Peterson low- and high-noise models [7]. Right: plot of the VSR2 sensitivity as well as the coherence projection of seismic probes on the sensitivity.

seismic environment is necessary, as well as identification among the infrastructure machines of relevant sources of seismic noise reaching the detector's sensitive components. The work described hereafter is part of this effort.

During the months of June and July in 2010, a Güralp-3TD seismometer was stationed to monitor floor vibrations at various technical areas around the Virgo site, which host several infrastructure machines (i.e. water chillers, heaters, pumps, etc). The power spectra of the measured seismic data were examined, and several single sources were identified using correlation of the seismic data with synchronous records of the infrastructure machines working status (i.e. temperature monitors, voltage sniffers, etc). Then, seismic data were correlated with the synchronous record of permanent seismic probes close to the detector. Studying the calculated coherence and power spectra, we selected 'relevant' sources whose noise emissions reach the detector and measure the noise attenuation between the sources and detector. We also measured approximate noise reduction factors as a function of the distance between the machine and the detector.

Section 2 discusses the methods used when taking and analyzing data. Section 3 describes examples of noise emissions from the sources found in this analysis at various locations. Section 4 provides an estimate for the attenuation of the noise spectral peaks as a function of distance. Section 5 presents our conclusions.

2. Characterization methods

2.1. Measurement setup

We acquired several sets of data with a Güralp CMG-3TD tri-axial seismometer [8] at six locations around the site. The Güralp CMG-3TD is a portable three-component broadband seismometer with a flat velocity response over the 0.0083–100 Hz frequency band. The chosen sampling rate was 250 Hz. The Güralp seismometer is equipped with a GPS antenna receiver

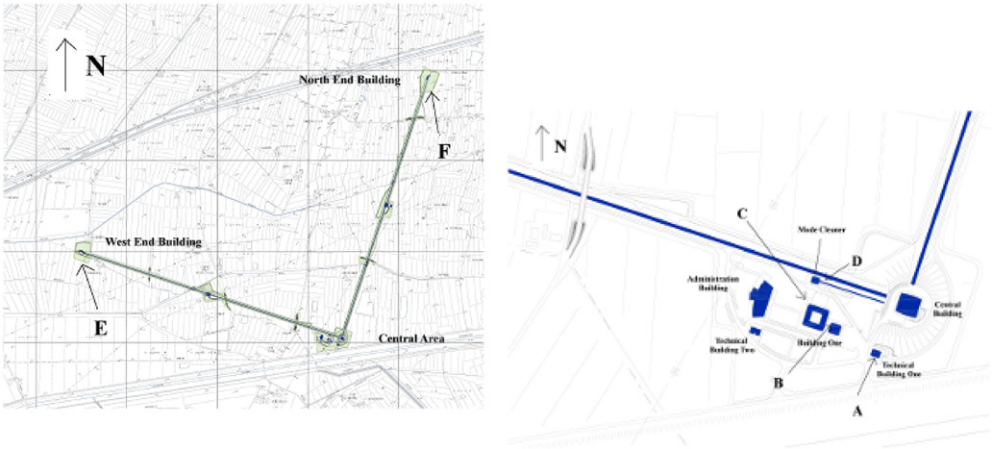

Figure 2. Left: aerial view of the Virgo interferometer. Right: aerial view of Virgo's central area. Measurement sites are marked with letters (see table 1).

Table 1. Locations of seismometer placement.

Section letter	Test probe location	Reference probe location	Distance between seismometers (m)
A	Technical Building 1: ground floor	Central Building: ground floor	80
B	Building 1: first floor	Central Building: ground floor	105
C	Outside Building 1: ground floor	Mode Cleaner: ground floor	30
	Outside Mode Cleaner Building: ground floor	Mode Cleaner: ground floor	10
E/F	West/North End Building: ground floor	West/North End Building: external optical bench	20

to synchronize its data to Virgo seismic channels. Maps for the site and the locations of the measurements can be seen in figure 2. These locations were chosen for their proximity to machinery known to create large seismic noise. These locations are detailed in table 1. At each location, the Güralp seismometer was installed on the same concrete platform where the machinery sat and if possible, at a distance of at least a few meters from the machinery to prevent saturation. For each location, the power spectral density (PSD) of the Güralp seismometer, referred to as the 'test probe', is computed (see figure 1 (left)). Each measurement lasts approximately 24 h in order to determine the hourly and daily cycle operation of the machines. This measurement is compared with a tri-axial seismometer, referred to as the 'reference probe', permanently stationed in the closest nearby experimental area containing sensitive interferometer components [6]. In the Mode Cleaner, West End, and North End buildings, the reference probe was an Episensor FBA ES-T, while in the Central building, the probe was a Güralp CMG-T40. The Güralp CMG-T40 is a three-component broadband seismometer with flat velocity response over the 0.05–50 Hz frequency band, while the Episensor FBA ES-T is a

Table 2. Important noise lines identified in the study. The line's frequency, periodicity, source, and the ratio of the PSDs of the test and reference probes are given.

Location	Frequency (Hz)	Periodicity (period)	Source	PSD ratio
Technical Building 1	24.2, 48.4,78.6	Periodic (42 min)	Cold-water chiller 1	16
Building 1	19.3	Continuous	Computer fans	13
Outside Building 1	48.9	Continuous (daytime)	B1 chiller	2
Mode Cleaner	48.9, 97.8	Periodic (21.5 min)	Mode Cleaner chiller	220
West End Building	47.1	Continuous	Warm-water pump	1.1
West End Building	48.8	Continuous	Cold-water pump	6.1
North End Building	22.8	Continuous	Water pump	4.2

three-axis velocimeter with a flat response over the 0.1–200 Hz frequency band. If the source is not obvious, suspected machines are analyzed with a piezoelectric accelerometer placed in direct contact with the machine and read out with a spectrum analyzer. This piezoelectric accelerometer is a PCB model 393B12 single-axis accelerometer with flat response in the range from 1 Hz to 1000 kHz. The machines characteristic frequencies are then compared to those seen in the coherence.

2.2. Analysis methods

We considered the relevant frequency lines (persistent spectral peaks) that appear as significantly coherent (coherence rising out of the background) between the test and the reference probes, as the source of those lines is very likely to be the same. Coherence itself does not allow one to distinguish between the seismic signals generated close to the test probe (i.e. machinery under test) from those produced close to the reference probe (i.e. cooling fans of electronic units). In order to determine when the former is the case, the ratio of the test and reference seismometers PSDs is examined, and coherent lines that are stronger near the reference probe are selected. These techniques work well for machines producing continuous lines, such as water pumps and cooling fans.

Periodic lines, on the other hand, are more difficult to identify. Because the lines come and go, they tend to be washed out in PSD averaging. For this reason, the frequency–time plots of the PSDs are produced and examined by eye for periodic lines. In order to identify the source of these lines, we compute the root mean square (RMS) around that line, which is defined as

$$\mathrm{RMS} = \sqrt{\sum_{i=f_1}^{f_2} x_i{}^2 * \delta f}, \tag{1}$$

where x_i is the ith component of the frequency band in question and δf is the width of the frequency bins in the spectrum. The sum goes from $i = f_1$ to $i = f_2$, where f_1 and f_2 are the minimum and the maximum frequencies, respectively, in the frequency band. This RMS value is then correlated with the time series of various infrastructure machine-monitoring system (IMMS) signals, including temperature and pressure probes.

3. Characterization examples

In this section, the most significant examples utilizing methods discussed above are presented. In table 2, information about important, identified noise lines are given.

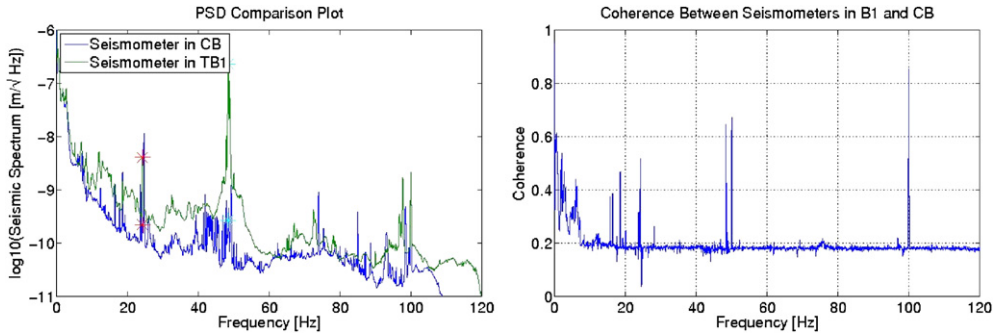

Figure 3. Left: PSDs of the seismometers in TB1 and CB. The peaks topped with red stars correspond to the 24.2 Hz periodic line, while the blue stars correspond to the 48 Hz continuous line. Right: coherence between seismometers in TB1 and CB. The peak topped with the red star corresponds to the 24.2 Hz periodic line, while with the blue star corresponds to the 47.9 Hz continuous line.

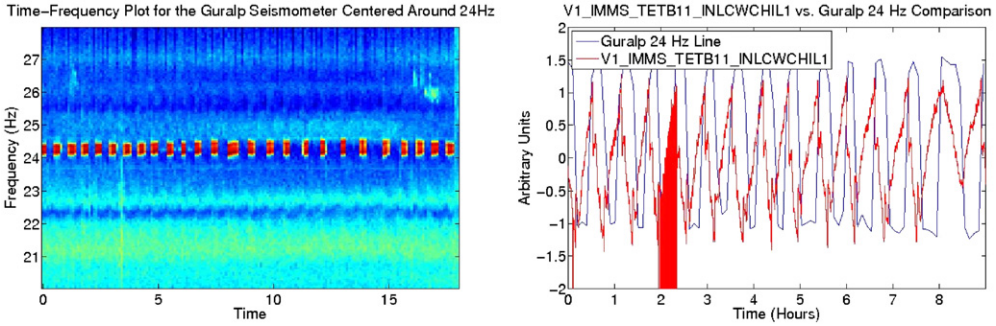

Figure 4. Left: the frequency–time plot of the test probe in TB1 zoomed in on the 24 Hz region. Right: a plot of both the RMS in the 24 Hz band of the Güralp seismometer as well as the time series of a temperature monitor of the first (of two) cold-water chillers.

3.1. Characterization of noise from Technical Building 1

A data set was taken in Technical Building 1 (TB1) and compared with data from a seismometer on the floor of the Central Building (CB), where the two arms of the interferometer converge. These two probes are approximately 80 m apart. The PSDs of the test and reference probes, as well as the coherence between them, can be seen in figure 3. A periodic line around 24.2 Hz (with harmonics at 48.4 and 72.6 Hz) is seen, which is shown in detail in figure 4 (left).

The coherence for this line between the test and the reference probes was about 0.6, indicating a relevant correlation between the two seismometers at that frequency. In order to find the source of the periodic line, it was necessary to determine in which building the line was louder. The ratio of the PSDs (seismometer in TB1/seismometer in CB) was approximately 16, indicating the source of the line to be in TB1.

The time series of several machinery monitors in TB1 were compared with the RMS of the 24.2 Hz signal in the Güralp seismometer, one of which can be seen in figure 4 (right). From this figure, the RMS is clearly correlated with the time series of a temperature monitor

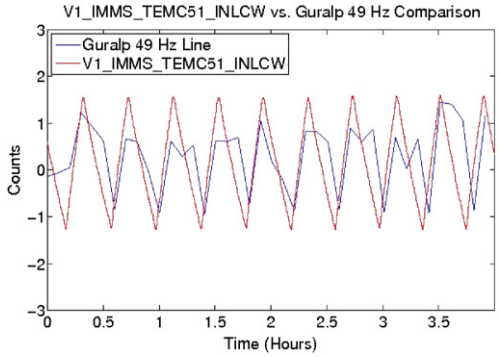

Figure 5. Comparison between the RMS in the 48.9 Hz band of the Güralp seismometer and the time series of a temperature monitor of the water chiller.

of the first water chiller. We see that when the temperature of the water reaches a high point, the cold-water chiller switches on, causing the temperature of the water to decrease. When the temperature reaches a low point, the water chiller switches off and the whole process starts again. The chiller is located on the roof of TB1. Even though the chiller is equipped with insulating springs, the vibrations can probably travel through the rigid water pipes between TB1 and CB or in the water itself.

3.2. Characterization of noise from the cold-water chiller outside the Mode Cleaner

Another data set was taken outside the Mode Cleaner Building (MCB), on the same concrete platform as the MC's cold-water chiller, and compared with the seismometer on the MCB floor. The MCB contains the end mirror of the Input Mode Cleaner, an optical cavity that filters jitter and power noise as well as higher order modes from the beam. The distance between these probes is approximately 10 m.

In viewing the PSD plots, a number of significant lines are noticed. This includes continuous lines at 24.2 and 38.8 Hz and a strong periodic line at 48.9 Hz, which has a harmonic at 97.8 Hz. To study this line, the RMS around the 48.9 Hz band was computed and compared to probes inside the MCB. A water temperature probe follows this line well, as can be seen in figure 5, indicating its source is the MC water chiller. This line is important since coherence was noted at its frequency between the GW channel of VSR2 run data and the seismometer in the MCB (see figure 1 (right)). Thus, it seems that the MCB water chiller affects the Virgo sensitivity and, for this reason, requires prompt attention for noise reduction.

3.3. Characterization of noise in the West End Building

Another data set was taken inside the West End Building (WEB) near the machinery and compared with an Episensor seismometer located on the external optical bench. The distance between these seismic probes is approximately 20 m.

Analyzing the PSD plots, we noted several significant lines, including continuous lines at 24.7, 47.1 and 48.8 Hz. 47.1 and 48.8 Hz are associated with the 'warm'- and 'cold'-water pumps, respectively, as verified with the piezoelectric accelerometer in figure 6. As the 47.1 Hz signal reached the optical bench with almost no attenuation, there is likely a preferred path, e.g., through water pipes, which must be investigated further.

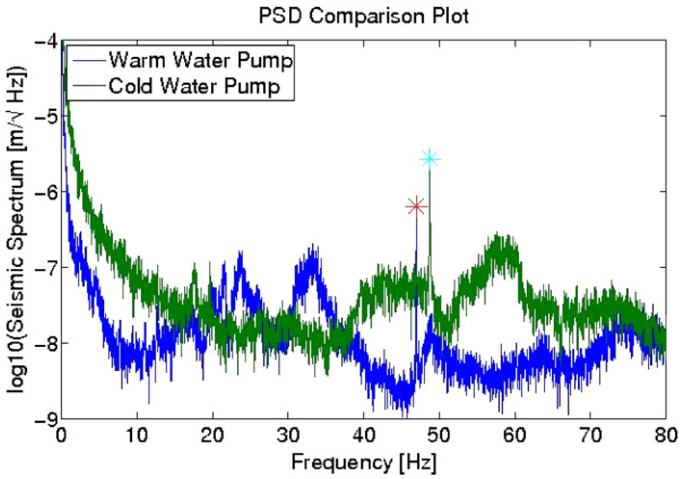

Figure 6. This plot shows the PSD for both the warm- and cold-water pumps in the WEB. The data were taken with the piezoelectric accelerometer in direct contact with the machines under study. The warm-water pump's PSD has a strong line around 47.1 Hz, which is shown by the red star on the left. The cold-water pump's PSD exhibits a strong line around 48.8 Hz, which is shown by the blue star on the right.

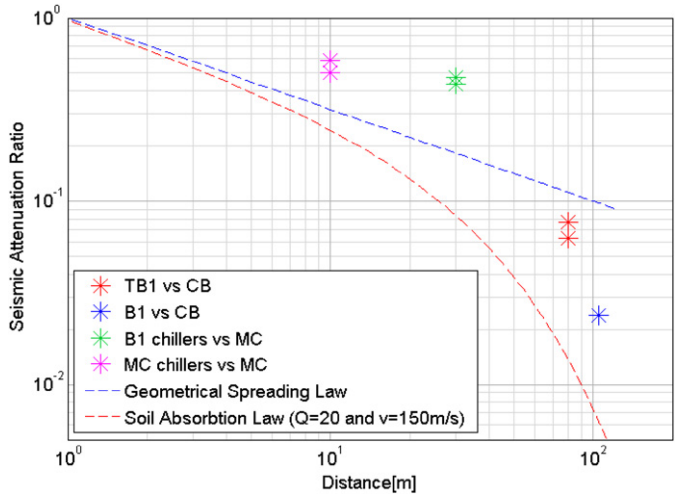

Figure 7. A plot of the average of the PSD ratio of the coherent lines as a function of distance between the probes. The soil quality factor ($Q = 20$) and phase velocity ($v = 200\ \mathrm{m\ s^{-1}}$) of surface shear waves have been measured at Virgo, as reported in [9]. We selected locations separated by at least a few wavelengths of soil. The attenuation factors data at 105 m are lower limits only.

4. Attenuation measurement

Using the above results, we seek to measure how much noise attenuation occurs when a machine is on its own foundation and a certain distance away from an experimental area. The PSD ratio of test and reference probes is used as a tentative estimate of the attenuation of the vibration, the result for which can be seen in figure 7. Measurements are compared to

a dissipation law accounting for geometrical spreading of surface cylindrical waves and for energy dissipation in soil (see [9] and references therein).

As can be seen in the plot, distances of about 30 m or less have an attenuation of approximately a factor of 3, while distances of about 80 m and greater have attenuation values greater than 10. Indeed, the simple noise attenuation model does not apply in most of the examined cases. One reason is that the point-like source approximation is not valid for short propagation distances ($d \leqslant \lambda$, with our seismic waves length $\simeq 10$ m) or for extended sources ($L \geqslant d$, with the machine platform size $L \simeq 10$ m). In addition, the soil medium is often not uniform, and waves' reflection and refraction can occur at discontinuities. Wave amplification due to mechanical resonances of the two platforms (technical and experimental areas) which are excited by the seismic noise is also possible. Another important reason is that in most cases propagation does not occur uniquely through soil. Less-dissipative paths can exist, such as through water pipes or pressure waves inside the water itself.

5. Conclusion

Noise from several Virgo infrastructure devices, such as water chillers, heaters, and pumps, seismically affects sensitive parts of the interferometer. Although an impact on the present interferometer is not evident in Virgo's sensitivity (with the exception of the MC chiller), the noise reaching the experimental area is, in several cases, considerably above the background and requires a reduction for the AdV.

Measured attenuation of seismic signal from a distant source seems not compatible with the much stronger attenuation expected from soil dissipation. It is suspected that water pipes might function as seismic shortcuts and thus need more comprehensive investigation and mitigation attention. Noise transmitted through soil can be more efficiently reduced using seismic isolation systems (i.e. springs).

Further beneficial studies might include setting up a noise source with the known power and characteristic frequencies at various distances from a sensitive experimental area. This would allow a comprehensive study of the noise attenuation as a function of distance, something we were unable to do in this study.

Acknowledgments

This project was funded by the NSF through the University of Florida's IREU program. The authors acknowledge the support from Italian Ministero dell'Istruzione, dell'Universita' e della Ricerca through grant PRIN 2007NXMBHP.

References

[1] Abbott B *et al* (LIGO Scientific Collaboration) 2009 *Rep. Prog. Phys.* **72** 076901
[2] Acernese F *et al* (Virgo Collaboration) 2008 *Class. Quantum Grav.* **25** 114045
[3] Braccini S 2005 *Astropart. Phys.* **23**
[4] Acernese F *et al* (Virgo Collaboration) 2008 *Virgo Internal Report VIR-0089A-08* (https://tds.ego-gw.it/ql/?c=2110)
[5] Accadia T *et al* (Virgo Collaboration) 2010 *Class. Quantum Grav.* **27** 194011
[6] Barone F, Garufi F and Milano L 2001 *VIRGO Document* VIR-MAN-NAP-5800-102 (https://tds.ego-gw.it/ql/?c=800)
[7] Peterson J 1993 *Open-File Report* 93–322
[8] Boschi V and Gennai A 2010 *VIRGO Document* VIR-0172A-10 (https://tds.ego-gw.it/ql/?c=7305)
[9] Saccorotti G *et al* 2011 *Bull. Seismol. Soc. Am.* **101** 568–78